

# IRIS 3 Program: Study of the Vibrations Induced by a Missile Impact on a Reinforced Concrete Structure

Nicolas VAN DORSSELAER<sup>1</sup>, Tess LEGAUD<sup>1</sup>, Vincent LAPOUJADE<sup>1</sup>, Benjamin RICHARD<sup>2</sup>

<sup>1</sup>DynaS+, Toulouse, France

<sup>2</sup>Institut de Radioprotection et de Sûreté Nucléaire, Fontenay-aux-Roses, France

## 1 Introduction

The IRIS program (Improving Robustness assessment of structures Impacted by a large missile at medium velocity) consists in an international benchmark under the hospice of OECD/NEA. After two first phases of this benchmark realized in 2010 and 2012 which aimed at assessing the ability of numerical simulations to describe the experimental structural response of the mock-up when subjected to impacts, the IRIS Program is now in its third phase. The main objectives of this phase are to assess the effect of a local damage caused by a missile impact on the induced vibrations and to assess the propagation of these vibrations to other parts of the structure, especially to pseudo-equipments which are anchored on it.

## 2 Data, Assumptions and Modeling

The third phase of the IRIS Program consists in reproducing by numerical simulation a set of impact tests on a reinforced concrete mock-up. The specimen is supported by four steel pipes, with two pseudo-equipments anchored inside (see figure 1). The test sequence is composed of three successive impacts of highly deformable 50 kg missile at a speed around 100 m.s<sup>-1</sup>.

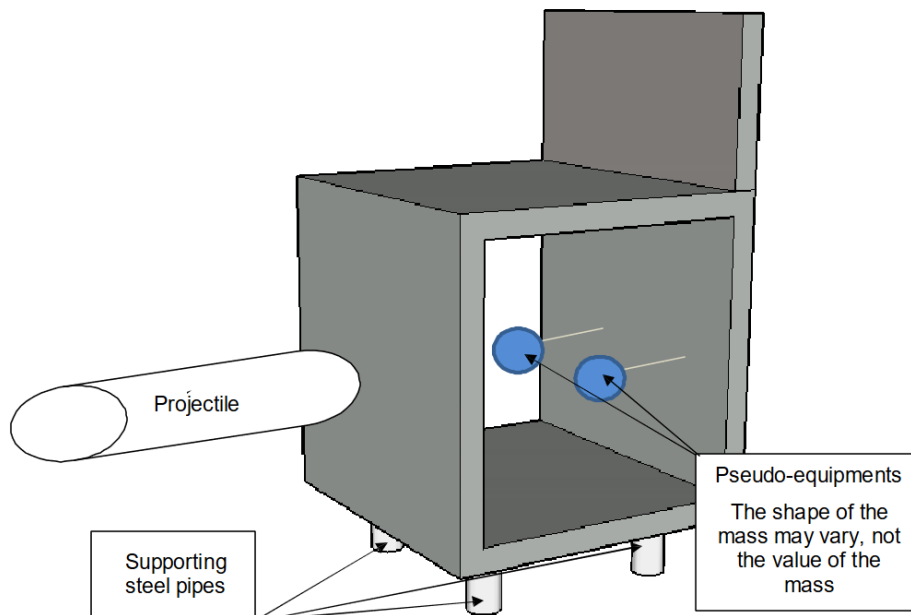


Fig.1: Principle of the experimental test [9]

The dimensions of the mock-up are approximately 2.5 x 3.5 x 2 m<sup>3</sup>. The concrete walls have a thickness of 0.15 m, excepted for the floor for which the thickness is equal to 0.4 m. They are reinforced by longitudinal and transverse rebars with a diameter of 6 mm or 10 mm.

A three-dimensional model has been developed for this mock-up with under integrated hexahedral solid elements for concrete, with an average mesh-size of about 0.025 m. Rebars are explicitly modeled with Huges-Liu beam elements, which are immersed in the concrete elements with the keyword `*CONSTRAINED_BEAM_IN_SOLID`. The following figures show some views of the concrete and rebars meshes.

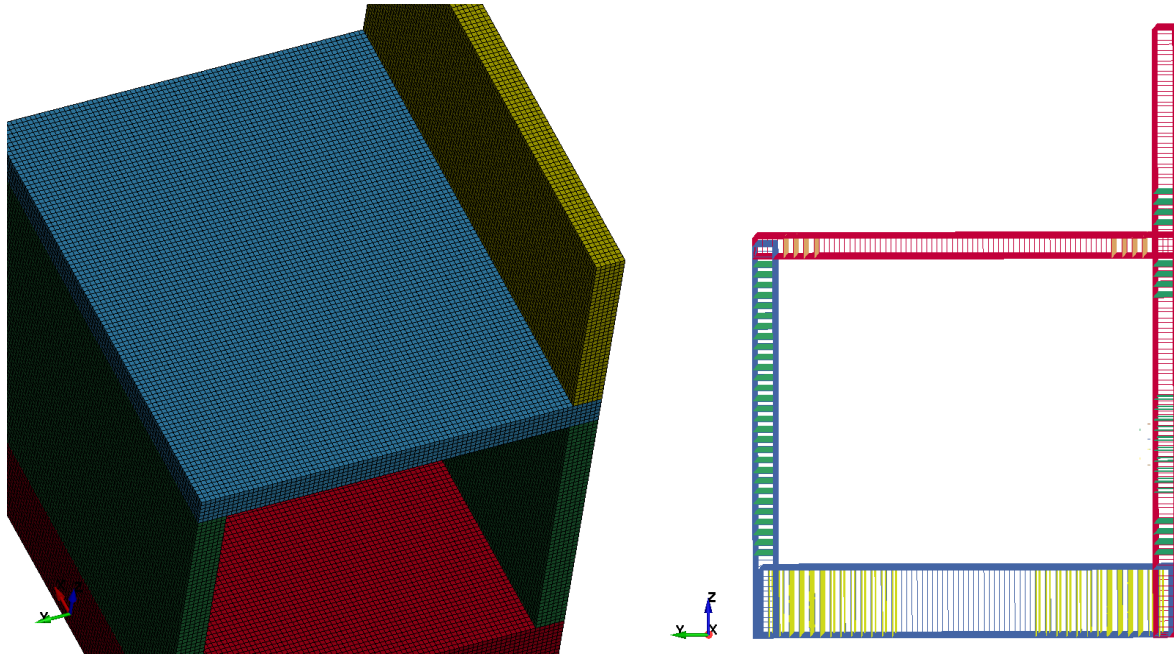


Fig.2: Views of the concrete mesh and the rebars

The pseudo-equipments anchored to the rear wall of the mock-up are constituted by two cylindrical masses of 60.7 kg linked to the wall by IPE beams and attached (one is bolted and the other one welded) to plates embedded into the concrete. Cylindrical masses are modeled with solid elements and are considered as rigid parts, IPE and plates are modeled with deformable shell elements. The welded connection is considered merged to the model and the bolted connection is modeled by deformable shells and `*CONSTRAINED_NODAL_RIGID_BODIES`. The following figures show a view of these pseudo-equipments modeling and their associated characteristic length (in meters) distribution.

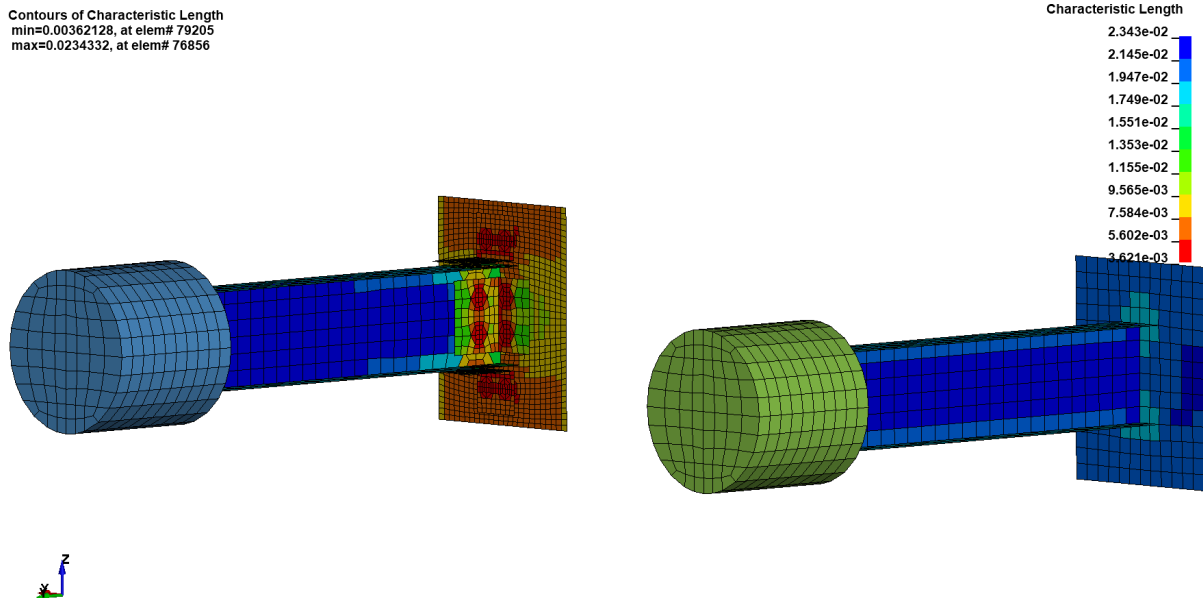


Fig.3: View of the modeling of the two pseudo-equipments

The steel supports are constituted by an empty cylinder with four stiffeners, a fixed bottom plate and a top plate embedded in concrete. These supports are modeled with shell elements. The following figure shows a view of the supporting steel pipes meshes and their associated characteristic length (in meters) distribution.

Contours of Characteristic Length  
 min=0.0130696, at elem# 383755  
 max=0.0299922, at elem# 382682

Characteristic Length  
 2.999e-02  
 2.830e-02  
 2.661e-02  
 2.492e-02  
 2.322e-02  
 2.153e-02  
 1.984e-02  
 1.815e-02  
 1.645e-02  
 1.476e-02  
 1.307e-02

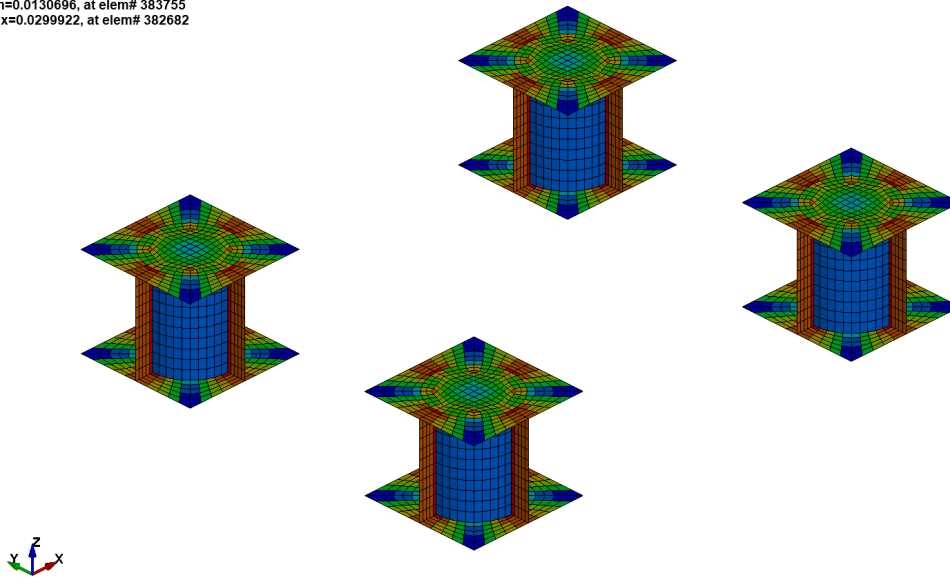


Fig.4: View of the supporting steel pipes meshes

The missiles are mainly constituted by a dome and a 2 m long steel pipe with a 2 mm thickness wall. They are meshed with shell elements with 1 cm element length to allow a good representation of buckling during the impact. The following figure shows a view of the missile mesh.

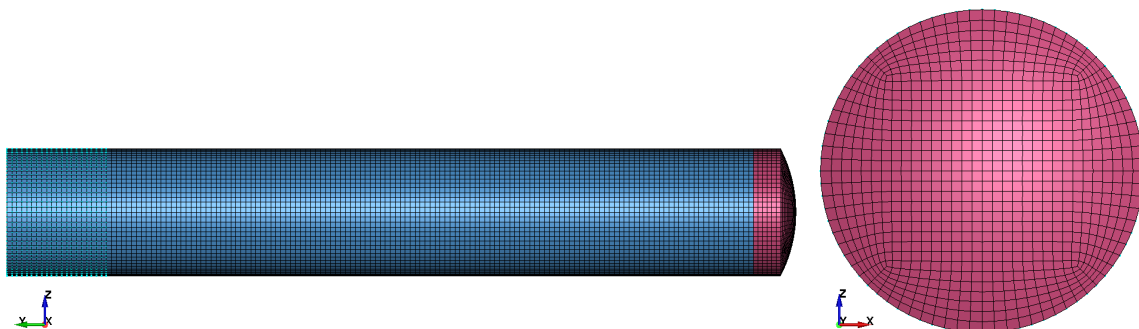


Fig.5: View of the modeling of a missile

Except for the cylindrical masses that are considered as rigid parts, all the steel materials are modeled using a **\*MAT\_PIECEWISE\_LINEAR\_PLASTICITY** including stress/strain curves from a quasi-static experimental tension test. For the concrete parts, experimental data from unconfined compressive tests and brazilian tests were available for the benchmark. From these values, several constitutive material laws using automatic parameter generation have been tested in this study:

- **\*MAT\_PSEUDO\_TENSOR** (16),
- **\*MAT\_CONCRETE\_DAMAGE\_REL3** (72R3),
- **\*MAT\_WINFRITH\_CONCRETE** (84),
- **\*MAT\_CSCM\_CONCRETE** (159),
- **\*MAT\_RHT** (272).

Considering the boundary conditions, all the nodes of the bottom plates of the steel supports are fixed in translation and rotation.

This study consists in performing three successive missile impacts on the same mock-up. A method using **\*INTERFACE\_SPRINGBACK\_LS-DYNA** has been used to initialize stresses and deformations from the end of an impact to the beginning of the following one. For each missile impact calculation, a

phase of impact of 0.15s is followed by a damping phase of 0.1 s using `*DAMPING_PART_MASS` using a critical damping factor calculated from the lowest natural frequency of the structure.

### 3 Results

#### 3.1 Modal Analysis

A numerical modal analysis of the mock-up has been performed. The objective is to compare the numerical model eigenfrequencies with the ones experimentally identified during hammer tests.

Here is a table of the comparison between numerical and experimental eigenfrequencies obtained with simple elastic material and linear element formulation for concrete parts.

Mode Number	Experimental eigenfrequencies (Hz)	Numerical eigenfrequencies (Hz)	Error (%)
1	17.50	24.57	40.4
2	30.20	55.22	82.8
3	44.30	58.85	32.8
4	45.80	63.19	37.2
5	48.70	65.67	34.8

Table 1: Comparison of 5 first eigenfrequencies between simulation and experiment

Numerical eigenfrequencies are overestimated. However, as it is shown on the following figure, the mode shapes obtained numerically are consistent with the experiment.

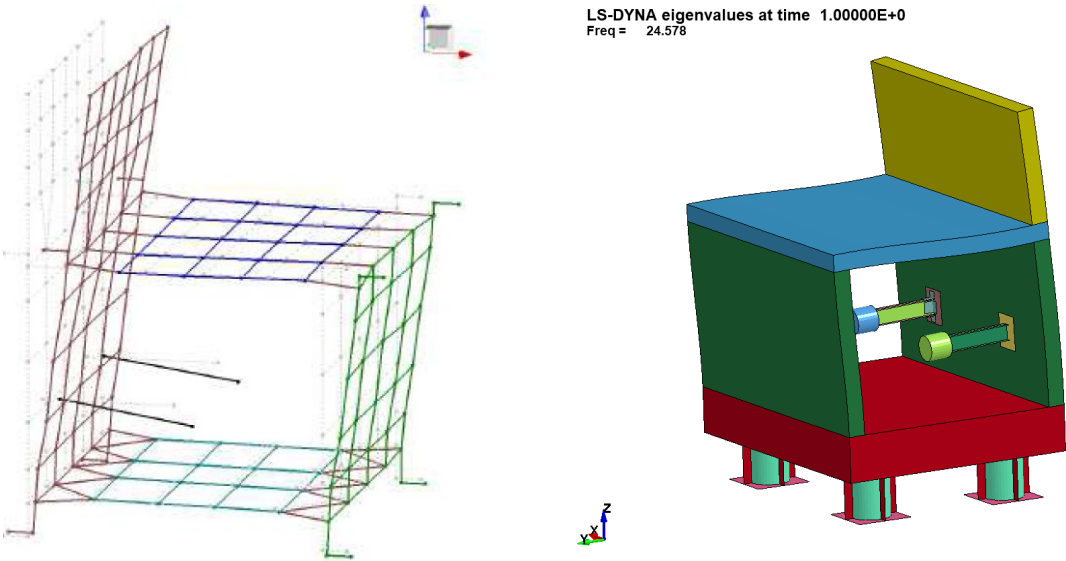


Fig.6: Comparison of the 1<sup>st</sup> mode shape between experiment (left side) and simulation (right side)

Several reasons may explain these results from the modal analysis. In the numerical simulation, the boundary conditions are modeled by fully constrained degrees of freedom which probably corresponds to stronger conditions than the experimental ones. Moreover, the modulus used in the model come from experimental tests on specimens, and we are not sure of the representativeness of these values compared to real concrete (mock-up walls are bigger and dryer than the specimens).

### 3.2 Missile impact calculations

Three successive missile impact calculations have been performed on the mock-up. They all give acceptable energy balance with a transformation of the initial kinetic energy in internal energy, and a conservative total energy. In all calculations, numerical energies like the Hourglass energy in the concrete walls and the contact energy are small regarding the internal energy.

The first two impacts being very similar (same missile with same velocity), only the results from the first impact and the third one (more energetic missile) are presented in this paper.

Results of this section are based on the model that uses the law `*MAT_CONCRETE_DAMAGE_REL3` for concrete parts. It is the model that minimizes the error for the maximum deflection of the impacted wall and the error of the maximal displacement of the pseudo-equipments.

For all cases, during the impact, the missile buckles in contact with the front wall of the mock-up and rebounds. The energy is transmitted to the walls and to the pseudo-equipments by vibrations induced by the impact. The observed deformations are very low, so as the vibrations, as it can be seen on the following figure.

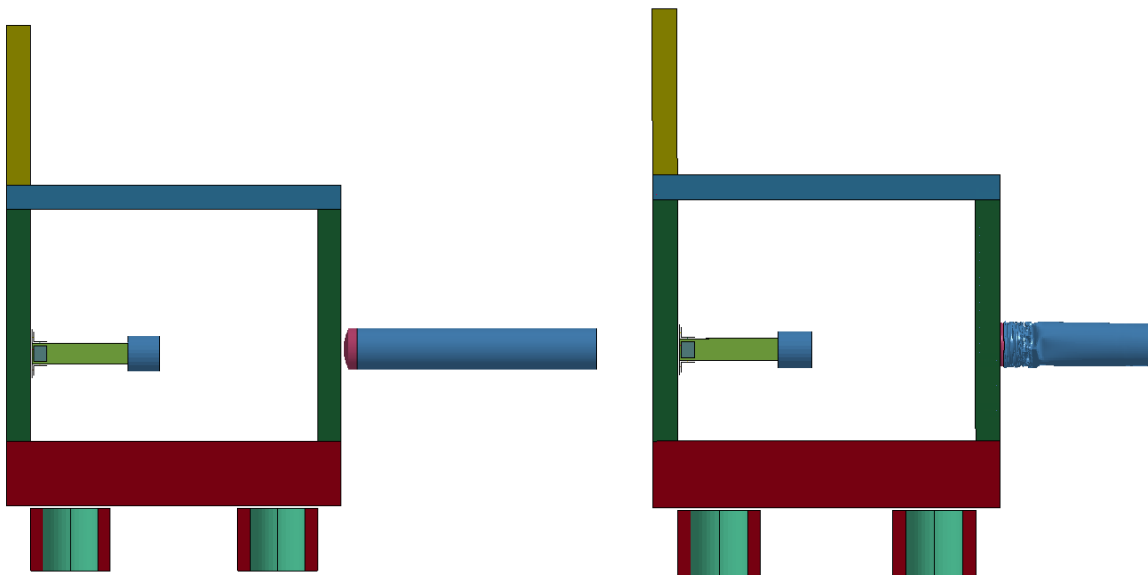
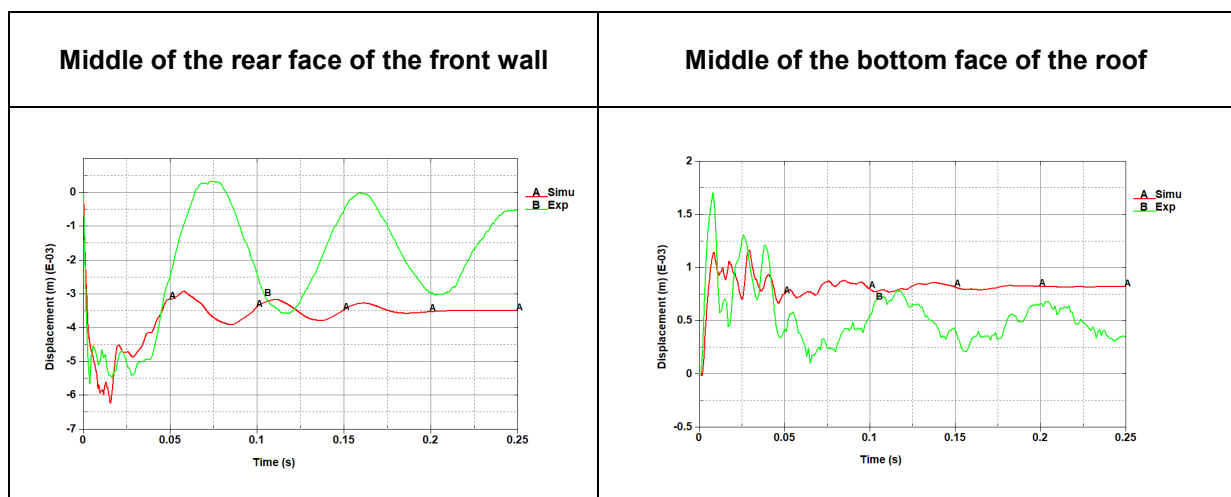


Fig.7: Views of the structure before the impact (left side) and at the end of the impact (right side)

Several sensors are put on the concrete walls in order to compare the vibrations induced by the impacts. The following figure presents a comparison of the displacement of the walls during the first impact at several locations between experiment.



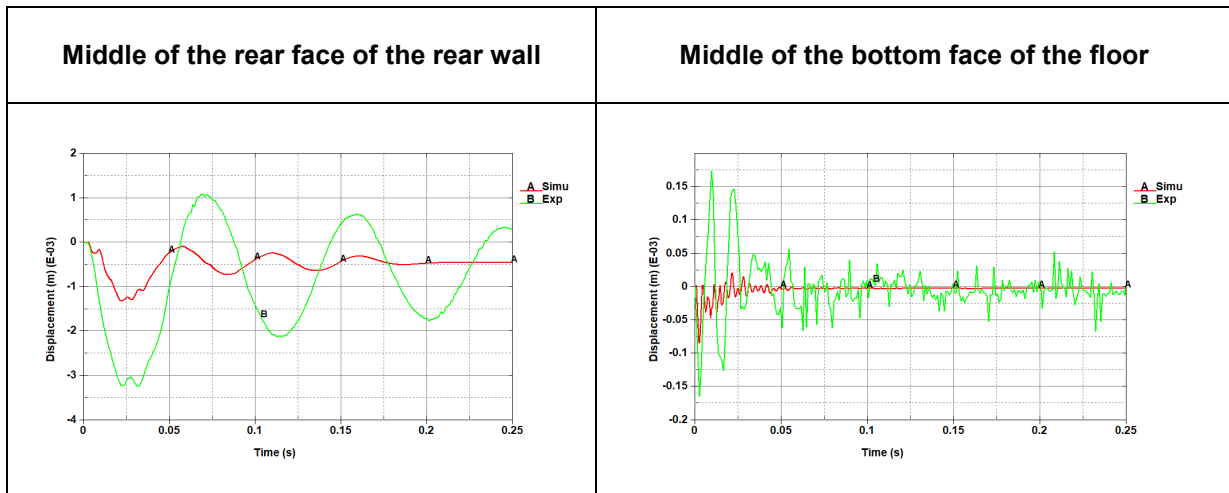


Fig.8: Displacement versus time evolution - first impact at several locations – experimental/numerical comparison.

Displacements obtained numerically at the front wall and the floor show a good agreement considering the maximum value but overestimate the residual value at the end of the impact. Moreover, the oscillations numerically observed show higher frequencies than the experiment, which is consistent with the conclusion from the modal analysis.

The displacement of the floor is much lower than in the experiment. This is also consistent with the conclusion of the modal analysis: the boundary conditions of the simulation are probably too perfect to reproduce the experiment.

The displacement of the rear wall is twice less important than the experimental displacement, and the oscillation frequency is too high. It seems that the numerical mock-up is stiffer and does not transmit the vibrations as well as the experimental one.

Regarding the displacement of the pseudo-equipments, a comparison between numerical and experimental oscillations can be made for the first impact (see following figure).

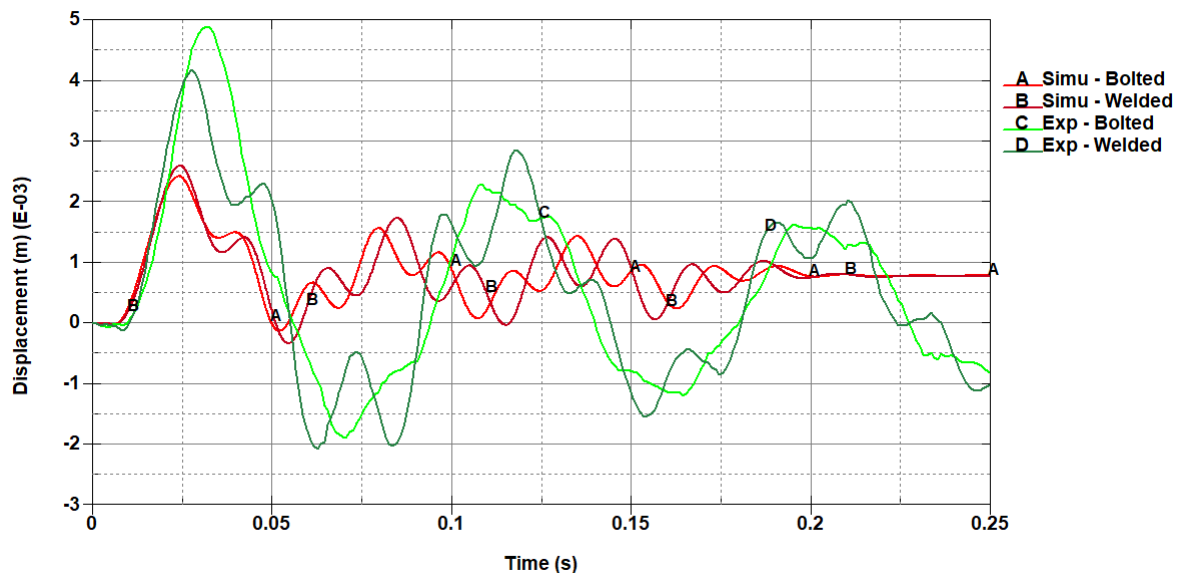


Fig.9: Comparison of the oscillations of the pseudo-equipments for the first impact between numerical simulation and experiment

The maximum amplitudes numerically obtained for the pseudo-equipments are about twice lower than the experimental ones. As observed previously for the walls, the oscillation frequencies are much

higher than in the experiment. In addition to the reason given before (the numerical mock-up is probably stiffer), the numerical pseudo-equipment may also be stiffer than the experimental one.

Concerning the damage and deformation of the front wall, we observe only very small plastic strains in rebars at the end of the first impact, located at the impact location and at the transition between the front wall and the floor. As an indication of the concrete damage of the front wall, we can observe the lambda value of the `*MAT_CONCRETE_DAMAGE_REL3` accessible in the history variable #6 (see following figure). This damage value is computed internally as a function of the effective plastic strain, the strain rate enhancement factor, and the pressure. It is used in a function to interpolate the stress between the yield failure surface and the maximum failure surface, or between the maximum failure surface and the residual failure surface.

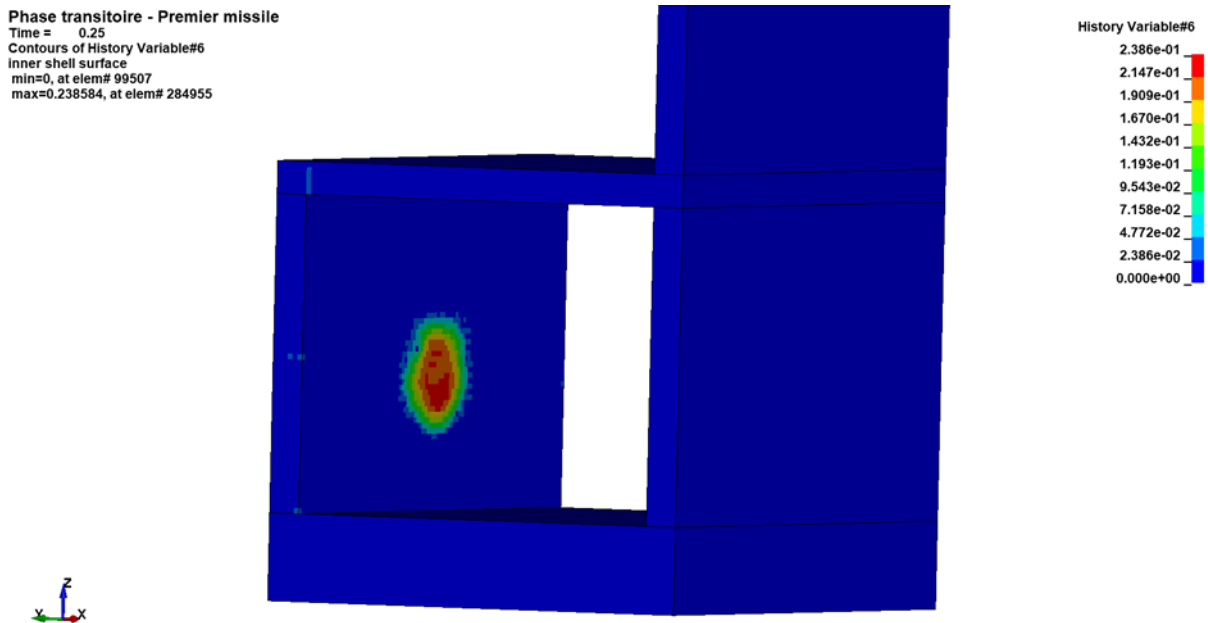


Fig.10: Lambda value in the concrete parts at the end of the first impact

The most damaged zone is located at the rear face near the impacted zone, because of tensile forces due to the reflection of the loading waves. The maximum lambda value is 0.239 which indicates a small damage.

For the missile, buckling is well reproduced in the simulation because the same number of folds as in the experiment is obtained (14 folds). The measurement comparison of folded and unfolded parts between the simulation and the experiment is shown in the following table.

	Experiment (mm)	Simulation (mm)	Error (%)
<b>Unfolded part</b>	749	713.6	-4.7
<b>Folded part</b>	160	211.5	32.2

Table 2: Comparison of deformed missile measurements between simulation and experiment

Folds number and unfolded part measurement show a good agreement with experimental results. However, folded part measurement has about 30% error compared to the experiment. This error comes from the mesh size chosen for the calculation (a compromise between accuracy and time calculation) that facetizes a little bit the folds.

For the third missile case, the impact velocity is twice more important than for the first ones, so the deformations and oscillations observed are more important than for the other impact cases. The following figure shows a comparison of the numerical and experimental deflection of the impacted wall during the third missile impact.

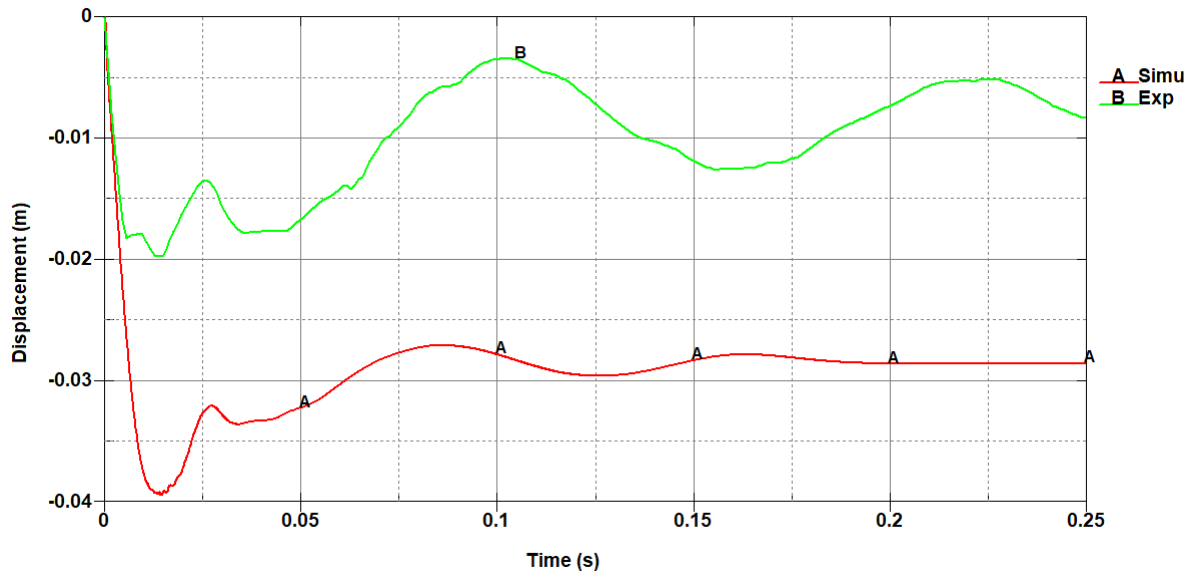


Fig. 11: Comparison of the numerical and experimental deflection of the impacted wall during the third missile impact

For the third impact, the numerical model highly overestimates both maximum and residual deflection of the front slab. This observation is confirmed by the damage obtained in the simulation on this wall (see final lambda value on the following figure).

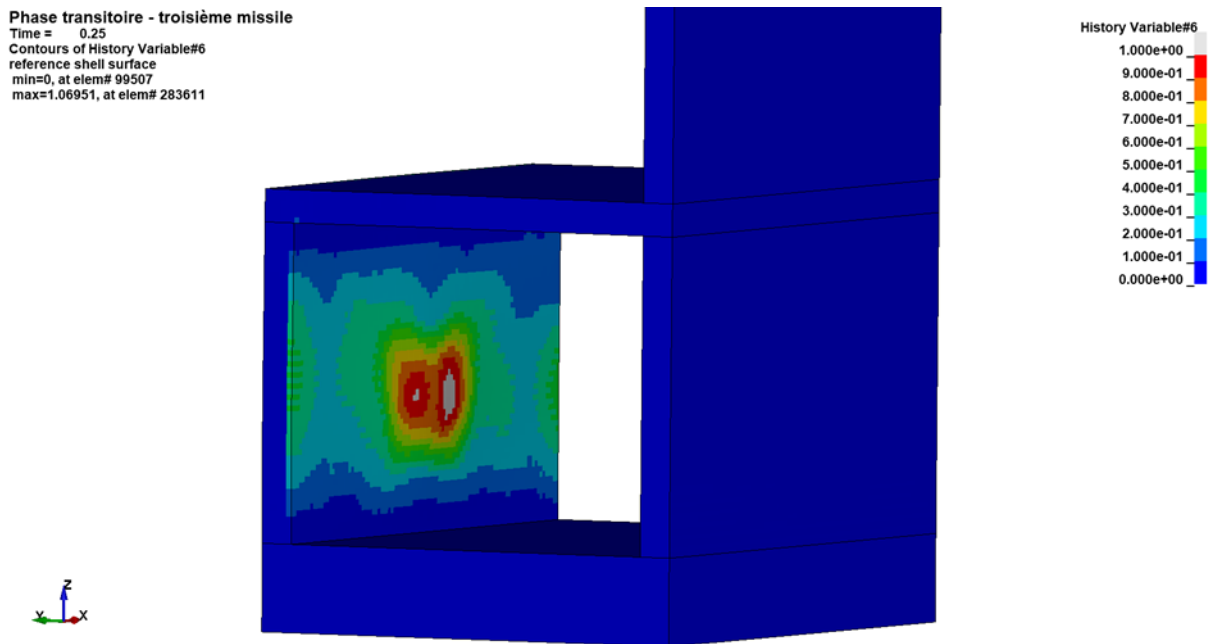


Fig. 12: Comparison of the numerical and experimental deflection of the impacted wall during the third missile impact

These results show a small damage on all the rear face of the front wall and a very high damage at the impact location (lambda value superior to 1). This is consistent with the experimental results because a lot of cracks appeared everywhere on this wall during the experiment. However, it seems that the chosen material law using parameters automatic generation locally overestimates the damage because in the experiment the concrete is not ruined behind the impacted zone.



Considering the vibrations of the pseudo-equipments induced by the third missile impact, the previous observations lead to little better reproduced oscillations than for the other impacts (see the following figure).

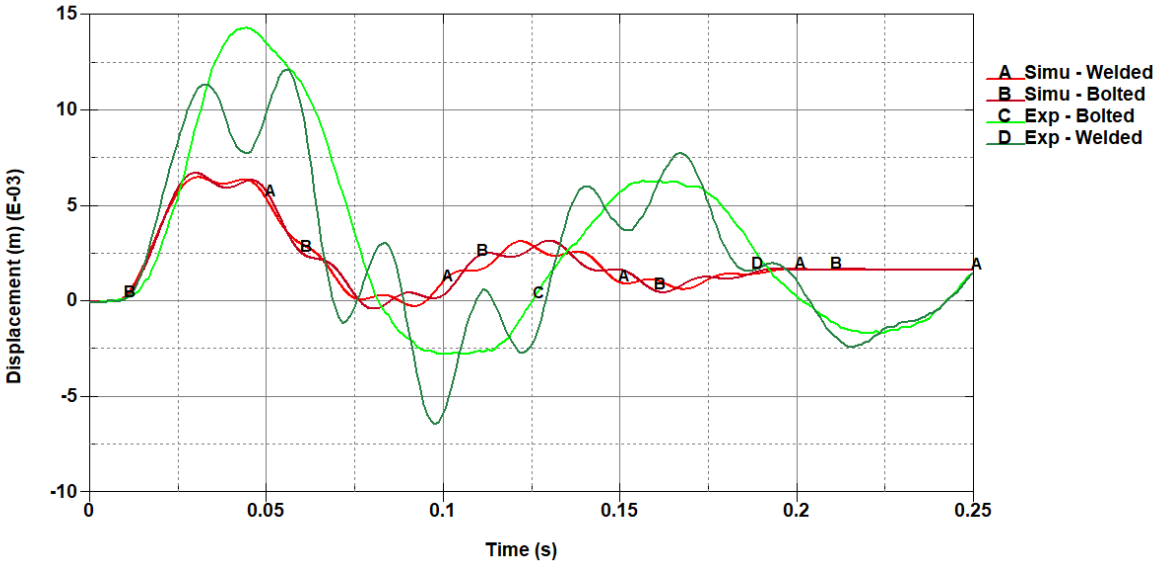


Fig.13: Comparison between numerical and experimental oscillations of the pseudo-equipments at the third impact

**4 Sensitivity Analysis**

A sensitivity analysis has been performed in order to find a way to reproduce the experimental results. Here is a list of the tests performed, all without a significant impact on the calibration of the model:

- modeling of the supporting steel pipes;
- modification of the shell element formulation used to model the IPE beams;
- modification of the beam element formulation used to model rebars;
- modification of parameters of pseudo-viscosity;
- modeling of the link for the bolted pseudo-equipment;
- modification of the mass damping factor.

Moreover, several constitutive laws have been tested for concrete parts. The following figures show the front wall deflection and one of the pseudo-equipments oscillations for all these laws compared to the experiment.

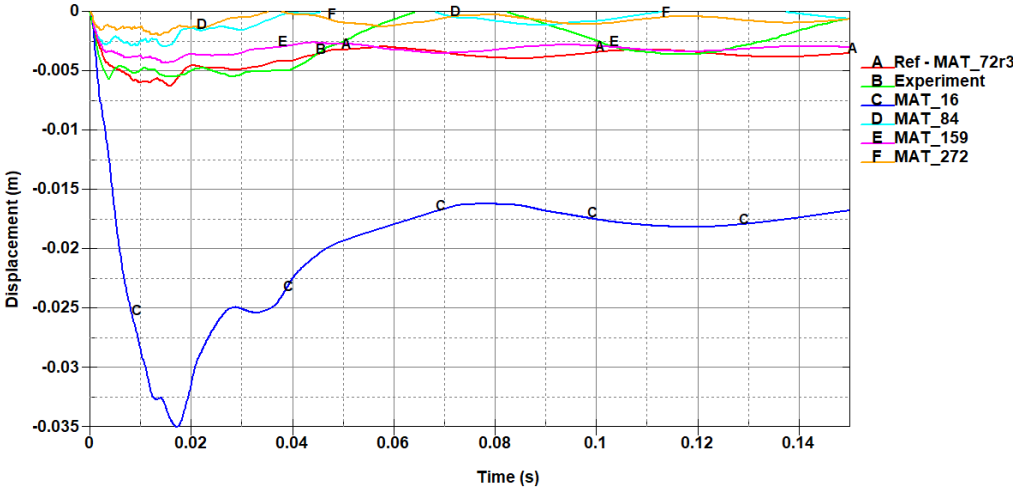


Fig.14: Comparison between numerical and experimental deflection of the front wall for all the material laws

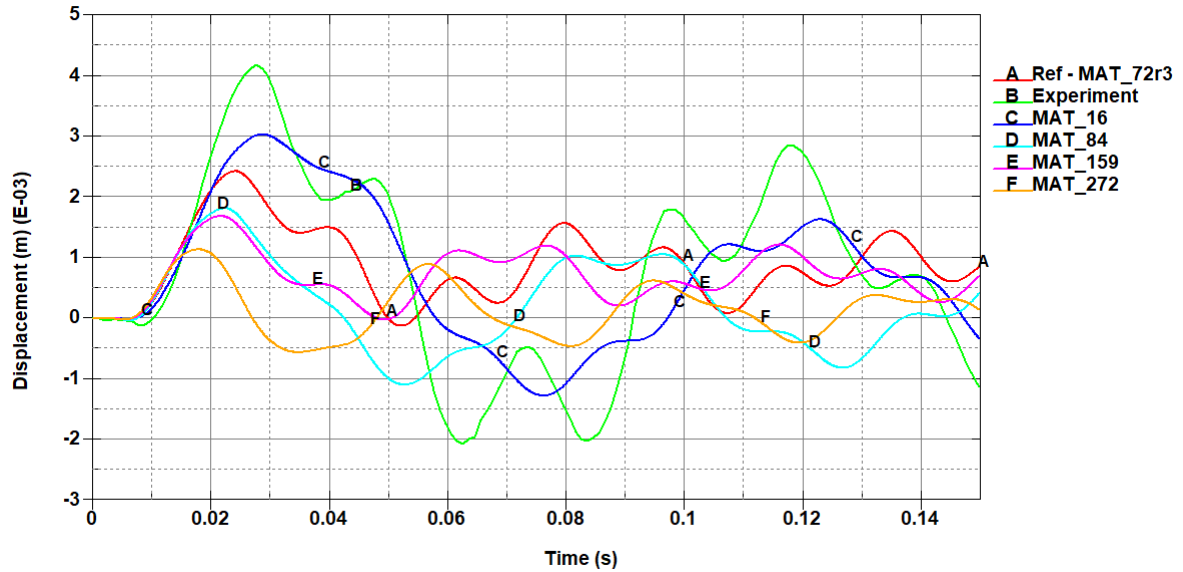


Fig.15: Comparison between numerical and experimental oscillation of the bolted pseudo-equipment for all the material laws

\*MAT\_16 seems to give similar pseudo-equipment oscillations as the experiment but it also gives a very high damage on the front wall correlated to a highly overestimated deflection. \*MAT\_272 highly underestimates all the displacements in this case. \*MAT\_84, \*MAT\_72r3 and \*MAT\_159 obtain a similar type of results with reduced oscillations of the pseudo-equipment compared to the experiment. In this study, \*MAT\_72r3 has been finally chosen for the final model because it is the one which minimizes the error on the maximum deflection of the front wall and the maximum amplitude of the pseudo-equipment oscillations.

As a complement, the modal analysis and the missile impact simulations showed that the structure is stiffer than it should be. The concrete modulus used in the model comes from experimental tests on specimens, and we are not sure of the representativeness of these values compared to the mock-up concrete (mock-up walls are bigger and dryer than the specimens).

To investigate this assumption, a sensitivity analysis has been performed on the concrete modulus with a reduction of the initial one. The objective was to optimize this modulus in order to calibrate the modal analysis to better reproduce the eigenfrequencies of the structure. Finally, as it can be seen on the following table, a value of 40% of the initial modulus highly reduces the error between experiment and simulation.

Mode Number	Experimental Frequency (Hz)	Numerical Frequency (Hz)	Error (%)
1	17.50	16.37	-6.5
2	30.20	40.95	35.6
3	44.30	46.04	3.9
4	45.80	53.80	17.5
5	48.70	55.44	13.8

Table 3: Comparison of 5 first modes between simulation with 40% of the initial modulus and experiment

This calibration is confirmed on the results of the missile impacts calculation, obtained with a \*MAT\_WINFRITH\_CONCRETE with a modulus at 40% of the initial one. The following figure shows a comparison of the displacement of the pseudo-equipments for this case.

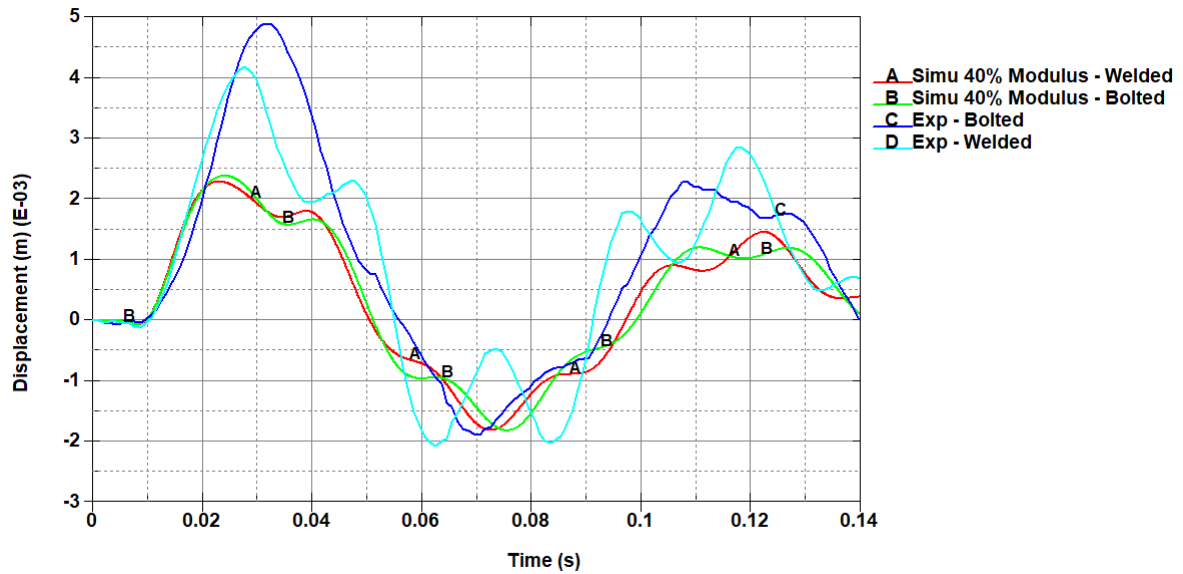


Fig.16: Comparison of the pseudo-equipments oscillations between simulation with 40% of the initial modulus and experiment

The oscillation frequency and the amplitude displacement for secondary oscillations are really improved compared to the reference results. However, even though this solution is numerically better, it is difficult to find a reason to justify such a huge reduction of the modulus. In fact, on a structure of this size, the concrete drying can't explain a 60% cut of the modulus.

## 5 Conclusion

This paper presented the results obtained by DynaS+ and IRSN during the third phase of the international benchmark IRIS Program. This phase aimed at performing three successive missile impacts on a reinforced concrete structure and at comparing the numerical results with the experimental ones.

The vibrations induced by the missile impacts and their propagation into the structure were very difficult to reproduce with numerical models because the numerical responses appeared to be stiffer than the experimental ones. Whatever the chosen material model tested for the concrete or numerical options are, LS-DYNA simulations are able to reproduce these vibrations with the good order of magnitude, but with an underestimation of the oscillations of the walls and the pseudo-equipments. Moreover, the vibrations in the numerical simulation always had a too high oscillation frequency, which is confirmed by the comparison between numerical and experimental modal analysis.

Even if a lot of parameters have been tested during sensitivity analysis, the only way found to improve the calibration of the numerical results was to highly reduce the concrete modulus. However, such a cut on the modulus is hard to justify because the values initially used came from material tests performed on specimens from the mock-up concrete batch.

As a following to this study, a future objective is to implement new material laws for concrete ([10]) in order to try to improve the concrete behavior for vibration applications.

## 6 Summary

The IRIS program (Improving Robustness assessment of structures Impacted by a large missile at medium velocity) consists in an international benchmark under the hospice of OECD/NEA.

The computation to be carried out by the participants aims at simulating three missile impacts at velocities around 100 m.s<sup>-1</sup> on a reinforced concrete mock-up fitted with two pseudo-equipment. The main objectives of the project are to assess the effect of a local damage caused by the impact on the induced vibrations and to assess the propagation of these vibrations to other parts of the structure and to the pseudo-equipment.

This paper presents the numerical simulation results obtained by DynaS+ and IRSN and a comparison with experimental results made available by the IRIS 3 program. A probabilistic approach has been set up for this study in order to identify the main parameters (dealing with material properties, local damage, boundary conditions, etc...) that have an influence onto the evolution of the shock inside the structure (in terms of magnitude, frequency domains and regarding different quantities of interest such as displacement, velocity and acceleration). After this step, the best options identified have been chosen to calibrate the numerical simulations based on the experiments. Regarding the results, a set of recommendations has been issued to perform this kind of numerical simulations by means of the LS-DYNA software.

## 7 References

- [1] Van Dorsselaer N., Lapoujade V., Nahas G., Tarallo F., Rambach J.-M.: "Impact Simulations on Concrete Slabs: LS-OPT Fitting Approach" – 8<sup>th</sup> European LS-DYNA Users Conference, May 2011, Strasbourg, France.
- [2] Van Dorsselaer N., Lapoujade V., Nahas G., Tarallo F., Rambach J.-M.: "General Approach for Concrete Modelling: Impact on Reinforced Concrete" – 12<sup>th</sup> International LS-DYNA Users Conference, June 2012, Detroit, USA.
- [3] Van Dorsselaer N., Lapoujade V., Nahas G., Cirée B., Tarallo F., Rambach J.-M.: "LS-OPT Parameter Identification on Concrete Samples Tests for an Impact Simulation on Concrete Slab" – 9<sup>th</sup> European LS-DYNA Users Conference, May 2013, Manchester, UK.
- [4] CEB-FIP Model Code 1990 – Comité Euro-International du Béton – 1990 – Thomas Telford House.
- [5] K&C Concrete Material Model Release III – Malvar, Crawford, Morill – Karagozian & Case – 2000.
- [6] LSTC, LS-DYNA Keyword user's manual Volume I, LS-DYNA R11, 18/10/2018.
- [7] LSTC, LS-DYNA Keyword user's manual Volume II – Material models, LS-DYNA R11, 12/10/2018
- [8] John O. Hallquist, LS-DYNA Theory manual, 03/2006
- [9] EDF, IRIS-3\_Overall\_Description-revD, 2017/11/15
- [10] Vassaux, M., Richard, B., Ragueneau, F., & Millard, A. (2015). Regularised crack behavior effects on continuum modelling of quasi-brittle materials under cyclic loading. *Engineering Fracture Mechanics*, 149, 18-36.